

Study on Seismicity and Seismic Tomography on a Hydrothermal System in West Java

Akhmad Fanani Akbar, Riskiray Ryannugroho, Philippe Jousset, Alexandra Gassner, Makky S Jaya, Rachmat Sule, Wahyuddin Diningrat, Andri Hendryana, Yosep Kusnadi, Andri Dian Nugraha, Muksin Umar, Yudi Indrinanto, Kemal Erbas

Faculty of Mining and Petroleum Engineering, Institut Teknologi Bandung, Indonesia

fanani_akbar@yahoo.co.uk

Keywords: tomography, seismicity, micro-earthquake, velocity

ABSTRACT

A total of 48 seismometers were deployed from October, 2012 to October 2013 around a geothermal field in the southern part of the Bandung basin region. A threshold time difference between S and P-wave was applied with an arrival time of less than three seconds. Otherwise, the waves were assumed as regional or teleseismic events. Then the P-and S-wave arrival times of events were carefully picked visually by eye. After this, the events were located. So far, 1,260 microearthquake events have been determined using a nonlinear algorithm integrated in the seismotool. These events seem to concentrated around geothermal field. Seismic velocities from the 1-D model were used as input for the 3-D seismic tomography inversion to invert for 3-D Vp, Vs, and Vp/Vs ratio subsurface structures around this geothermal field.

1. INTRODUCTION

Geothermal energy is one of the biggest energy sources in West Java. This is because geothermal energy in West Java has an important role for the energy potential in resources or reserves. Indonesia, located along the Ring of Fire in the Pacific Islands, has some of the largest resources of geothermal energy in the world. As much as 40% of the world's geothermal potential is found in Indonesia alone. The first step in determining the proven potential of a geothermal field is determining its reservoir boundary. In this study, a microseismic method was used to determine the subsurface character beneath a geothermal field in West Java. A network of 30 broadband and 4 short-period (1 Hz) seismic stations with Gürulp and Trillium sensors (0.008 – 100 Hz) were deployed from October 2012 until December 2013. This network was extended in June 2013 with 16 short-period seismometers.

Volcanic activity and plate movement can be determined by the distribution of earthquake locations. Besides that, the distribution of earthquake locations can be used for geothermal reservoir monitoring, especially for microearthquakes. The hypocenter determination of microearthquakes is influenced by the following: geometry of monitoring stations, error arrival time reading, phase waves availability, and geological structure knowledge in the study area (Gomberg et al, 1990). Before determining the hypocenter location, one has to identify what kind of earthquake it is. Most of the microearthquakes have low difference arrival time of P and S waves and have higher frequency content than regional earthquakes.

Linear inversion using Geiger's method was used to determine the travel time data faster. When applied to the field, there are weathering layer and topography effect that cannot be solved with this method. So, different joint hypocenter determination methods were used. This included determining the arrival time, travel time, hypocenter, station correction, and 1-D velocity model simultaneously. The result of Velest was used as input for tomography inversion to invert 3-D Vp, Vs, and Vp/Vs ratio subsurface structures around this geothermal field.

2. DATA

A seismometer network of 30 broadband and 4 short-period (1 Hz) seismic stations with Gürulp and Trillium sensors (0.008 – 100 Hz) was used from October 2012 until December 2013. This network was extended in June 2013 with 16 short-period seismometers that used Earth Data Logger (EDL) sampling at 200 sps and DSS CUBE data logger (Omnirecs) recording data with 200 sps. The P-and S-wave arrival times of events were picked manually to get high quality data. In this study, only the time difference between the P and S waves (ts-tp) that had values less than 4 seconds event were classified as microearthquake events. After that, the hypocenter locations were determined using Geiger's method that used homogen velocity. A total of 1767 microearthquake events were obtained in this study area. Most of the microearthquake events occurred in the exploited geothermal field and some structures. Moreover, 1072 events that occurred in May 2013 were located SW of the area of the exploited geothermal field.

3. METHODS

Determining the hypocenter location is one of the most fundamental analyses in earthquake studies. In many cases, hypocenter determinations often result in biases, where the locations are displaced from the true locations. Those biases possibly lead to wrong further analyses. To overcome those problems, Geiger's method was used to determine the initial hypocenter, joint inversion of hypocenter location, station correction, and velocity model using Velest, and joint inversion of hypocenter and velocity using tomoDD

3.1 Hypocenter location determination

This method used arrival times of P and S waves, stations location, and 1-D velocity model. The residual time is the difference between the observed and calculated arrival times, as shown in the equations below.

$$r_i = t_{obs}^i - t_{cal}^i \quad (1)$$

$$r_i = \left(\frac{\partial t_i^{cal}}{\partial x_i} \right) \Delta x + \left(\frac{\partial t_i^{cal}}{\partial y_i} \right) \Delta y + \left(\frac{\partial t_i^{cal}}{\partial z_i} \right) \Delta z + \Delta t_0 \quad (2)$$

Where,

r_i = travel time residual

t_{obs}^i = observation arrival times at station i

t_{cal}^i = calculation arrival times at station i

In this study, the GAD software program is used with Geiger's method with adaptive damping. If ordinary geiger is used,

$$G^T d = G^T G m \quad \text{. However, GAD uses } G^T d = (G^T G + \lambda I) m \quad \text{, where } G = \frac{\partial t_i^{cal}}{\partial x_i}, \frac{\partial t_i^{cal}}{\partial y_i}, \frac{\partial t_i^{cal}}{\partial z_i}$$

3.2 1D Velocity modeling

In this case, the velocity models used were 1-D models. This was done to simplify the subsurface models. The 1-D velocity model was used as a procedure to determine the hypocenter and as an initial velocity model for seismic tomography (Kissling et al., 1994). One of the methods used to determine the 1-D velocity model was the coupled velocity-hypocenter method using the VELEST software program version 3.1 (04/10/95) (Kissling, 1995).

VELEST can be used to solve problems such as:

1. The coupled hypocenter-velocity model problem for local earthquakes, quarry blasts, and shots; for fixed velocity model and station corrections VELEST in simultaneous mode performs the joint-hypocenter-determination (JHD).
2. The location problem for local earthquakes, blasts, and shots.

The coupled hypocenter-velocity method is a method of relocating earthquakes, seismic wave velocity model determination for subsurface 1-D, and correction stations simultaneously using the principle method of Geiger. The number of model parameters (m) is $5 + N$, (x, y, z, t_0 , station corrections, and N is the number of 1-D velocity model layers). As a first step, the parameters are defined with focal $m0$ (x, y, z, t_0), seismic wave velocity model (1-D), and station corrections. The next step is doing ray tracing of earthquakes to obtain T_{cal} (travel time calculation).

Inverse modeling can be used with the completing damped matrix least square approach [At $A + L$] (A = matrix Jacobi, Jacobi matrix A^T = Transpose; L = damping matrix). Using the value of damping will affect the value of the perturbation parameter model (Δm). The relationship between the magnitude of the damping and the value of Δm is the opposite.

Results of inverse modeling are in the vector of improved parameter model (Δm), which consists of the hypocenter, velocity model, and station corrections. In the next step, it is used in forward modeling as input. In the iteration, there is an RMS value between the observation and calculation travel times, so the iterations number can be set up to the expected RMS.

3.3 TomoDD

TomoDD combines both absolute and relative arrival time data. TomoDD determines a 3D velocity model jointly with absolute and relative event locations. Zhang and Thurber developed a double difference (DD) tomography code (tomoDD) based on the DD location code hypoDD that used simultaneous inversion for velocity structure and event locations.

TomoDD method is based on assumption that if the hypocenter between two earthquakes is less than the space between the earthquake and station, the ray path between the two earthquakes is identical. With this assumption, the time difference of both earthquakes recorded on same station can be a function of the space between the two earthquakes. It can decrease the value of the velocity error without using a station correction (Walshausen dan Ellsworth, 2000). Thus, the velocity results of tomoDD will be better than conventional tomography because when standard tomography is used, the hypocenter location is scattered. It is possible that errors come from picking the wrong arrival time for P and S waves and other sources. But using the travel time differential in the tomoDD method reduces errors from conventional tomography.

4. RESULTS

4.1 Initial hypocenter location

A network of seismometers of 30 broadband and 4 short-period (1 Hz) seismic stations with Guralp and Trillium sensors (0.008 – 100 Hz) were installed from October 2012 until December 2013. We extended the network in June 2013 with 16 short-period seismometers that use Earth Data Logger (EDL) sampling at 200 sps and DSS CUBE data logger (Omnirecs) recording data with 200 sps. We picked P-and S-wave arrival times of events manually to get high quality data. We found 1829 micro-earthquake events as well as 12302 P- and 12396 S-wave picks. Most of the events (1070 events) occurred in May 2013.

To determine hypocenter locations, we used a homogenous velocity model with a V_p of 3500 m/s and V_p/V_s 1.499 based on Wadati diagram (Figure 3). There are three clusters of micro-earthquake events and we determine boundaries for each cluster. The blue and red areas occur beneath the geothermal area, and so are related to the geothermal exploitation activity. At first we interpreted the blue area as occurring because of an intrusion, but when we tried to overlay the hypocenter locations with a residual gravity anomaly (Nasution et al., 1995) there was no correlation. So the blue cluster is not related to an intrusion. After that we tried to overlay it with structural geology map (Bahar, 2004), and found it clustered beneath the intersection of two fault (Figure 2). So,

the blue cluster is related to fault activity. We still need to find out why the fault movement is activated, but it seems it may be not related to geothermal activity because the first earthquake in this area started from the south-west to north east and it location lies in a different cluster.

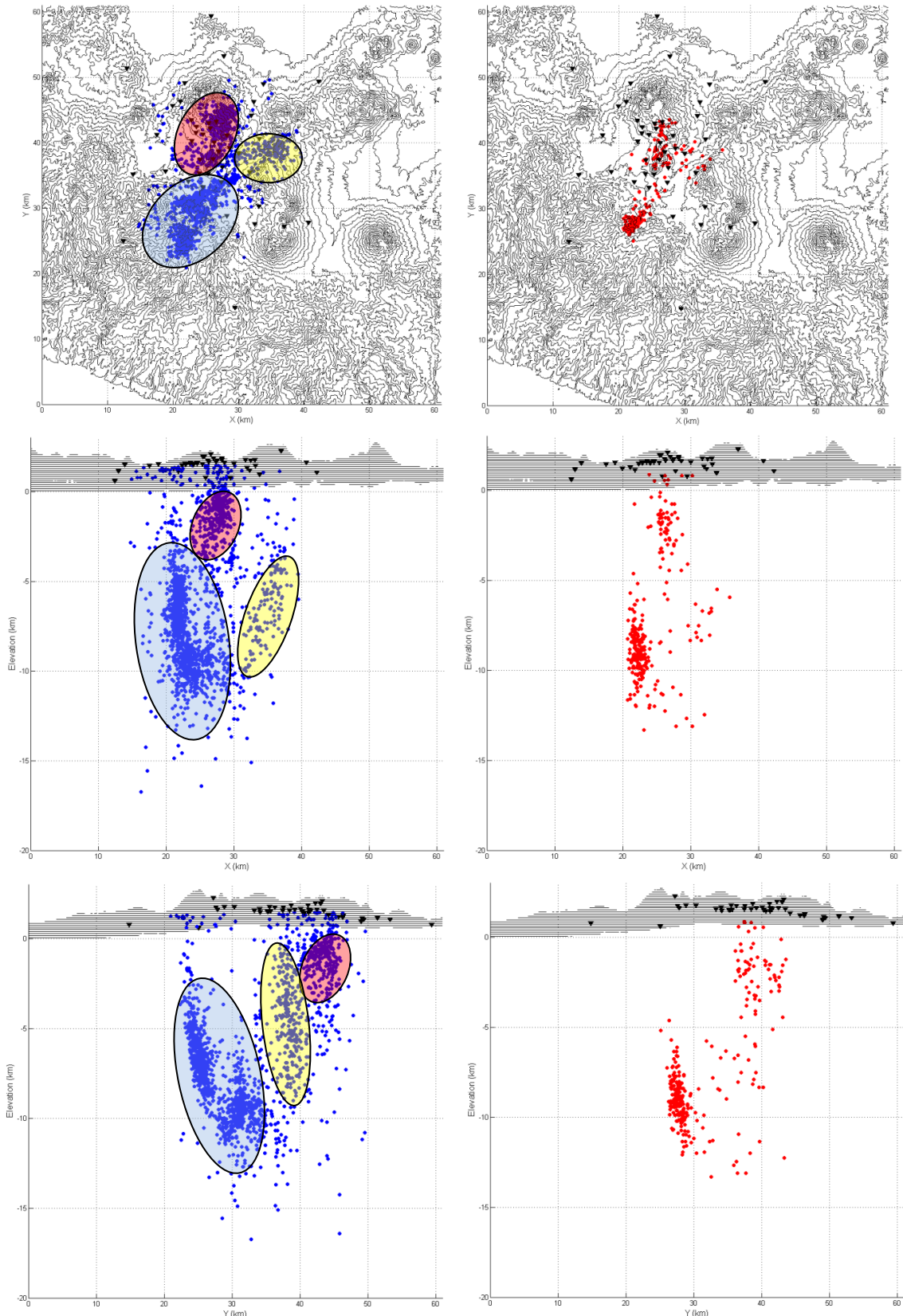


Figure 1. Distribution of micro-earthquake events in map view (top), vertical cross section along x-axis (middle), vertical cross section along y-axis (bottom) of micro-seismic hypocenter using Geiger's method (blue dot) and joint hypocenter determination metod (red dot) with station receiver (black triangle) and topography (black line). There are 3 clusters of micro-earthquake events: the blue and red area occur beneath the geothermal area and blue area occurs because of fault activity.

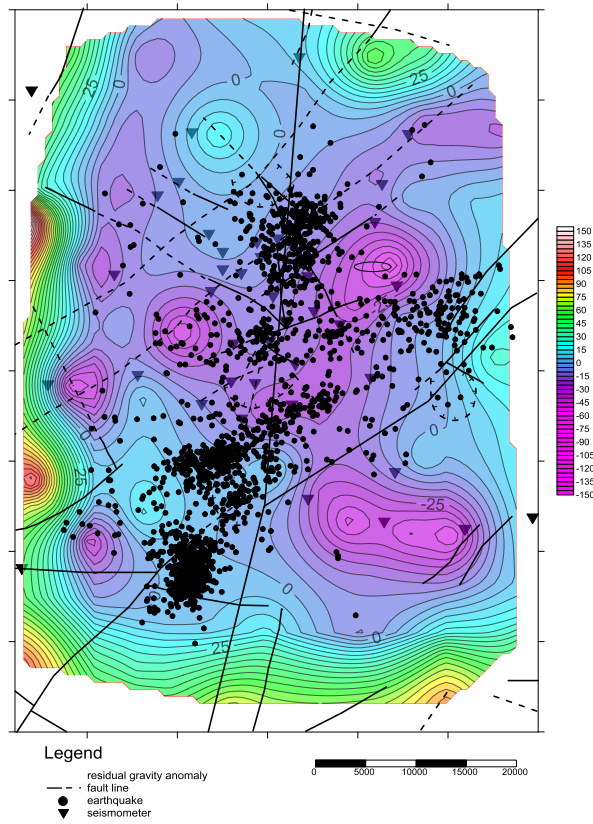


Figure 2: Overlay of fault line, epicenter location, and residual anomaly.

The RMS error lies between 0.075 and 0.25. Most of high error RMS events are in the blue area (Figure 1) because they occurred at the border of the seismometer network and in May 2013.

4.2 1-D velocity model

Results of the initial hypocenter location from Geiger's method, were used as input to the determined 1-D velocity model. However, not all the events were used. Only 465 events that had GAP less than 180 were used. In addition, from picking the arrival time for P and S wave, the Wadati diagram was created to determine the trend line of V_p/V_s in this study area. The Wadati diagram showed that the V_p/V_s in this area was 1.49 (Figure 3). This was used as an input parameter in Velest. Results from Velest included the hypocenter locations (Figure 1), 1-D model (Figure 4), and the station correction. The distribution of hypocenter locations was deeper than the result of Geiger's method and more clustered. RMS residual was decreased from 0.8 s to 0.19 s. Every station had the same value for station correction, for P it was 0.0 second and for S it was 0.2 second.

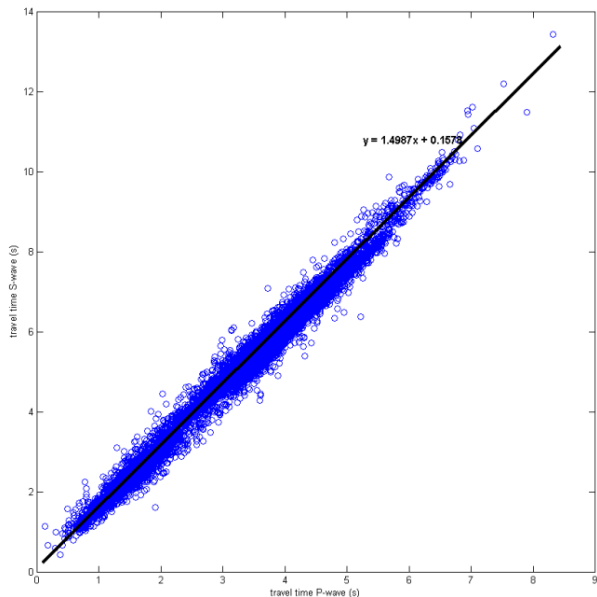


Figure 3. The Wadati diagram showing the trend line provides an average V_p/V_s ratio of 1.49

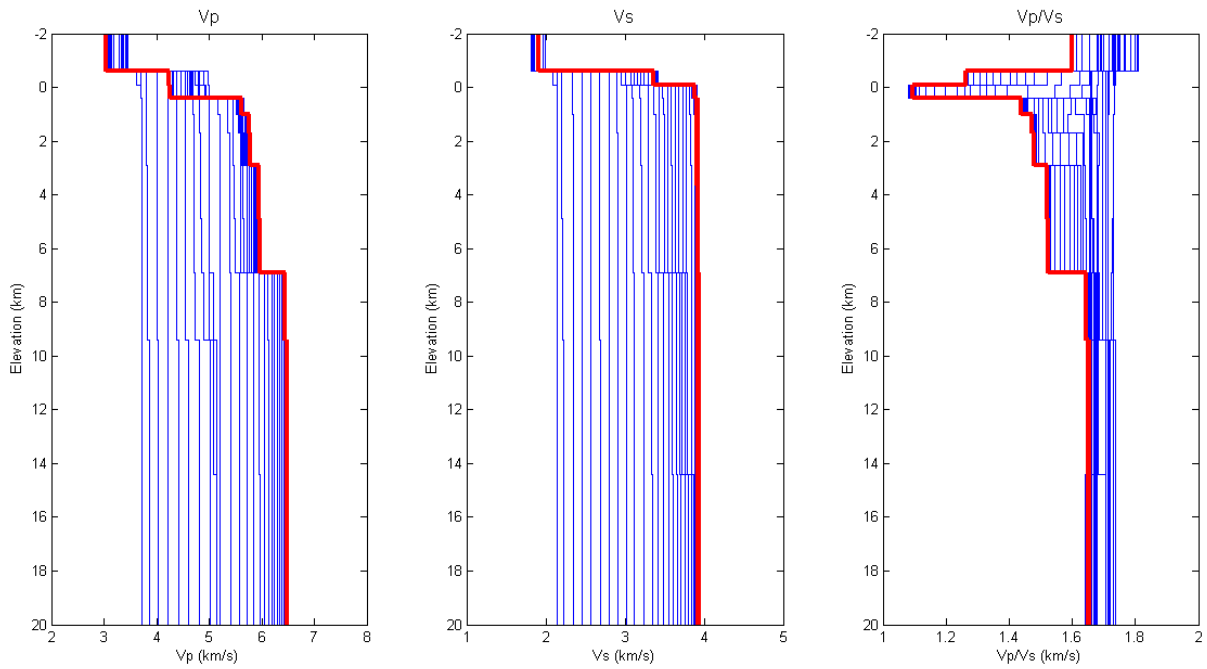


Figure 4. Results of 1-D velocity model inversion using Velest, showing P velocity (left), S velocity (middle), and Vp/Vs ratios (right).

5. CONCLUSION

We used 50 seismometers to monitor micro-earthquakes activity. There are 12302 P- and 12396 S-wave phase that can be picked in 1829 micro-earthquake events. Geiger's method is used to determine initial hypocenter locations and gave three clusters of events. Two clusters occur beneath two exploited geothermal areas and one cluster occurs because of fault activity. 1D velocity model is investigated with VELEST. There is a low anomaly of Vp/Vs beneath mean sea level, which indicates the location of a geothermal reservoir. We will add regional earthquakes to our catalog of data to determine deep subsurface conditions and to determine the relationship between subduction and geothermal systems. We will set up a 3D velocity tomography model and add some additional data (geophysics, geology, and geochemistry) to help us do an interpretation.

REFERENCES

Boitnott, G. N., and Kirkpatrick A., Proc. Twenty-Second Workshop on Geothermal Reservoir Engineering, Stanford University, Stanford CA (1997).

Gomberg, J. S., K. M. Shedlock, and S. W. Roecker, , The effect of S-wave arrival times on the accuracy of hypocenter estimation, *Bulletin of the Seismological Society of America*, **80**, (1990), 1605–1628.

Kissling, E., Ellsworth W.L., Eberhart-Phillips D., and Kradolfer U., *J. Geophys. Res.*, **99**, (1994), 19635-19646.

Kissling, E., Program VELEST USER'S GUIDE – Short Introduction, Zurich: ETH Zuerich, (1995), 1-31.

Nishi, K., Hypocenter Calculation Software GAD (Geiger's method with Adaptive Damping), *JICA report* , (2005).

Waldhauser, F. and Ellsworth, W.L., A Double-Difference Earthquake Location Algorithm: Method and Application to the Northern Hayward Fault, California, *Bulletin of the Seismological Society of America*, **90**, (2000), 1353–1368.